# From the Top: Surface-derived Carbon Fuels Greenhouse Gas Production at Depth in a Neotropical Peatland

Alexandra Hedgpeth[1,2], Alison M. Hoyt[3], Kyle Cavanaugh[1], Karis J. McFarlane[2*], Daniela F. Cusack[1,4,5*]

[1]Geography Department, University of California Los Angeles, Los Angeles, 94143, USA
[2]Lawrence Livermore National Laboratory, Livermore, 94550, USA
[3]Department of Earth System Science, Stanford University, Stanford, 94305, USA
[4]Department of Ecosystem Science & Sustainability, Colorado State University, Fort Collins, 80523, USA
[5]Smithsonian Tropical Research Institute, Balboa, Ancon, Republic of Panama, 0843-03092

★ These authors contributed equally to this work

*Correspondence*: Alexandra Hedgpeth (hedgpea10@g.ucla.edu)

**Abstract.**

Tropical peatlands play an important role in global carbon (C) cycling but little is known about factors driving carbon dioxide ($CO_2$) and methane ($CH_4$) emissions from these ecosystems, especially production in deeper soils. This study aimed to identify source material and processes regulating C emissions originating deep in three Neotropical peatland sites on the Caribbean coast of Panama. We hypothesized that: 1) surface derived organic matter transported down the soil profile is the primary C source for respiration products at depth; 2) high lignin content results in hydrogenotrophic methanogenesis as the dominant $CH_4$ production pathway throughout the profile, which relies on organic matter fermentation rather than carbon dioxide. We used radiocarbon isotopes to determine whether $CO_2$ and $CH_4$ at depth are produced from modern substrates or ancient deep peat, and we used stable C isotopes to identify the dominant $CH_4$ production pathway. Peat organic chemistry was characterized using ^{13}C solid state nuclear magnetic resonance spectroscopy (^{13}C-NMR). We found that deep peat respiration products had radiocarbon signatures that were more similar to surface dissolved organic C (DOC) than deep solid peat, even though the peat chemistry remained relatively stable from the surface to the deeper layers. These results indicate that surface derived organic matter was the dominant source for gas production at depth in this peatland, likely because of vertical transport of DOC from the surface to depth. Lignin, which was the most abundant compound (55-70% of C), increased with depth across these sites, whereas other C compounds like carbohydrates did not vary with depth. These results suggest that there is no preferential decomposition of carbohydrates, but preferential retention of lignin. Stable isotope signatures of respiration products indicated that hydrogenotrophic rather than acetoclastic methanogenesis was the dominant production pathway of $CH_4$ throughout the peat profile, suggesting dominance of respiration rather than fermentation for fuelling methanogenesis. These results show that deep C in tropical peatlands does not contribute greatly to surface fluxes of carbon dioxide, with compounds like lignin preferentially retained. This protection of deep C helps explain how peatland C is retained over thousands of years, and points to the vulnerability of this C should anaerobic conditions in these wet ecosystems change.

# 1 Introduction

Climate change is expected to disturb hydrological cycles in the tropics, with changes in rainfall regimes already observed for many tropical regions (Kharin et al. 2007, Feng et al. 2013, Magrin et al. 2014, Duffy et al. 2015, Chadwick et al. 2016, Barkhordarian et al. 2019). Changes in rainfall are of particular relevance to the storage of the 70 – 130 Gt of organic carbon (OC) stored in tropical peatland soils under anaerobic conditions, which could be under threat of rapid mineralization if rainfall declines and aerobic conditions emerge (Girkin et al., 2022; Loisel et al., 2021). Tropical peatlands store the largest pool of vulnerable and irrecoverable C of any ecosystem type, and this pool is sequestered over thousands of years (Goldstein et al., 2020; Noon et al., 2021). Despite their importance, tropical peatlands are logistically challenging environments to work in and are understudied compared to their northern counterparts, making tropical peatlands underrepresented in global C inventories (Ribeiro et al., 2021).

Peatlands sequester C as they build vertically with the oldest deposits at the base and less decomposed younger material accumulating at the surface (Clymo et al., 1998; Ingram, 1987). Despite temperatures ideal for microbial activity, the buildup of organic matter is possible because rates of primary production in the tropics exceed decomposition rates, which are low because peatland water tables are high (Nottingham et al., 2019; Page et al., 2011). Thus, deep peat is comprised of minimally processed plant material from the surface that accumulates due to anaerobic conditions, creating a globally significant buildup of C over time that could be metabolized if conditions became more favorable for decomposition (Hoyos-Santillan et al., 2019; Kettridge et al., 2015; Wilson et al., 2021). However, this age-depth relationship is not as straightforward in the tropics as in northern peatlands, because tropical peatland microtopography shows higher variability due to increased vegetation diversity and size, and forest disturbance can have dramatic effects on peat accumulation patterns (Dommain et al., 2015; Girkin et al., 2019). The dominant vegetation that acts as the stabilizing structure in early peat development, as well as the vegetation that serves as the biological origin of the peat itself, is also different in northern and tropical peatlands, leading to differences in peatland development, organic chemistry, and accumulation patterns between these two regions (United Nations Environment Programme et al., 2008).

Under current conditions, there is considerable variation in C emissions across tropical wetland systems (Farmer et al., 2011; Fritts, 2022), but some relationships have been generally characterized. It is mostly accepted that water table depth (Cobb et al., 2017; Hoyos-Santillan et al., 2019; Hoyt et al., 2019), temperature (Girkin et al., 2020; Hirano et al., 2009; Jauhiainen et al., 2014), substrate availability, and associated links with the dominant vegetation type (Upton et al., 2018; Wright et al., 2011, 2013), are strong controls on atmospheric emissions from tropical peatlands. Furthermore, surface vegetation plays an important role in the release of C by several processes, including being the biological origin of the peat matrix, which is composed primarily of lignin rich fibrous material in woody tropical peatlands, and determining labile C inputs in the form of decomposing plant tissues or root exudates (Girkin et al., 2018b; Lampela et al., 2014; Osaki et al., 2021). The majority of studies conducted in tropical peatlands have focused on the top 30 cm of the peat column; these depths are not only more accessible and easier to measure, but they are assumed to contribute the majority of emissions (Dhandapani et al.,

2022; Jauhiainen et al., 2005; Sjögersten et al., 2011). However, it is not known if the above drivers are mainly restricted to the surface, or if these processes influence $CO_2$ and $CH_4$ production deeper within the peat profile.

In many peatlands, microbial respiration across the soil profile can be supported by multiple C sources, and it is possible to use the radiocarbon signature of C respired from peatlands to partition sources into modern/surface dissolved OC (DOC) transported down the soil profile, versus older/buried solid C (Chanton et al., 2008; Hoyos-Santillan et al., 2016). Modern DOC, derived from surface vegetation, root exudates, and other recently photosynthesized organic matter, has a signature that is enriched in $\Delta^{14}$C. The existing peat and DOC from *in situ* decomposition of that deep peat, would have depleted radiocarbon signatures compared to the modern DOC (Girkin et al., 2018b; Wilson et al., 2016).

There have been several studies exploring the source of DOC used by microbes for respiration within peat soils. Most studies were from northern peatlands, and determined that respiration products were intermediate in their radiocarbon activity between newer surface DOC and *in situ* older C in peat (Aravena et al., 1993; Chanton et al., 1995, 2008; Charman et al., 1999; Clymo and Bryant, 2008; Elizabeth Corbett et al., 2013). Fewer studies have reported that respiration products are more similar to modern DOC radiocarbon signatures, demonstrating dominant use of surface DOC in deep peat gas production (Wilson et al., 2021). There is limited data from tropical peatlands, but two previous studies from the tropics have contrasting results; one shows intermediate respiration products (i.e., produced by mixed sources) in a tropical peatland in Borneo (Hoyt, 2014), and another shows modern, surface-derived inputs are the dominant source in sites across the Pastaza-Marañon basin in Peru (Hoyt et al., 2020). Potential explanations for this variable source contribution in tropical peatlands include differences in hydrology across sites, as well as the difference in dominant vegetation across the tropics. Biological origin can influence the chemistry and bioavailability of both modern DOC inputs and the resulting older peat (Dhandapani et al., 2023; Gandois et al., 2014), which could contribute to the different results reported for these two tropical peatlands with distinct surface vegetation.

Methanogenesis is an important pathway of decomposition in wetland systems. Acetoclastic methanogenesis is associated with acetate fermentation and the production of $CH_4$ from relatively labile organic compounds, while hydrogenotrophic methanogenesis is associated with $CO_2$ reduction, and can be supplied by the decomposition of more complex organic matter, with this second pathway less energetically favourable to microbes (Kotsyurbenko et al., 2004; Sugimoto and Wada, 1993). Metabolically, acetoclastic methanogenesis is more energetically favourable (i.e. more potential energy released), more efficient in $CH_4$ production, and generally results in higher rates of $CH_4$ production compared to hydrogenotrophic methanogenesis (Kotsyurbenko et al., 2004; Liebner et al., 2015). Shifts in $CH_4$ production pathways between acetoclastic methanogenesis and hydrogenotrophic methanogenesis occur depending on substrate availability, with acetoclastic favoured if fermentation products are available, as have been seen with depth in northern wetlands (Chanton et al., 2008; Corbett et al., 2013; Hornibrook et al., 2000). Changes in the availability of labile materials throughout the peat profile, even at depths of 2 meters, may be crucial not only for supplying the C substrate for $CO_2$ and $CH_4$ production, but also for influencing the mechanisms and quantities of $CH_4$ generated (Moore et al., 2013; Sun et al., 2012).

This study explored sources of soil surface C emissions, $CH_4$ production pathways, and organic carbon chemistry of peat in three sites in a Neotropical peatland in Panama. Previous work suggested that subsurface peat may contribute

125    substantially to net $CO_2$ and $CH_4$ flux from this peatland, but the source of C for these emissions was unclear (Wright et al., 2011). We used a combination of stable and radioisotope signatures of $CO_2$ and $CH_4$, and $^{13}C$ solid state nuclear magnetic resonance spectroscopy ($^{13}C$-NMR) characterization of peat soils, to identify the sources of the C gases produced in subsurface (>30 cm) peat. We hypothesized that: H1) surface-derived DOC is the primary C source for microbial respiration products at depth, where solid peat is more chemically complex and protected against decomposition. For this hypothesis, we predicted

130    that deep solid peat would have a higher decomposition index compared with surface peat. H2) Hydrogenotrophic methanogenesis is the dominant $CH_4$ production pathway at depth, resulting from decomposition of complex organic matter, rather than fermentation of more simple C compounds, which would support acetoclastic methanogenesis (Fig 1). We report and discuss radiocarbon analyses of subsurface DOC, $CH_4$, and $CO_2$ as well as peat biomolecular characterization using solid state $^{13}C$-NMR spectroscopy in a tropical peatland.
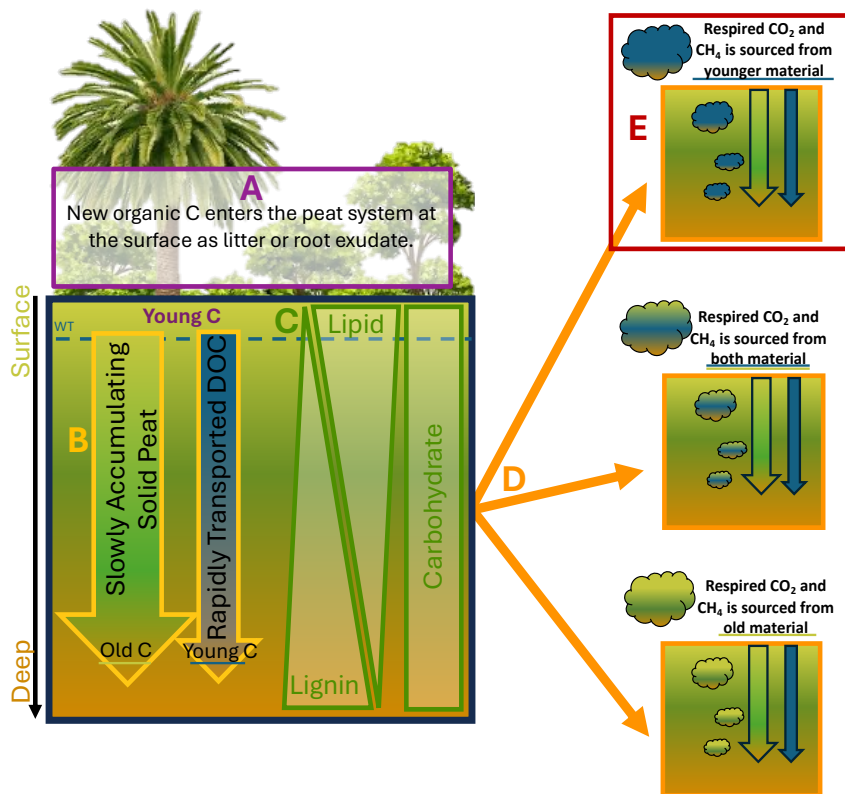
**Figure 1: Schematic illustrating our conceptual understanding of the tropical peat C cycle.** A) Surface vegetation acts as the primary source of new organic material entering the peat system. Key contributors include dead plant matter and root exudates, and lant species can influence the organic chemistry of C inputs to soils B) Slow accumulation of solid peat matter (green), versus the rapid fluxes of fresh, modern dissolved organic carbon (DOC) from the surface (blue) C) As bulk peat accumulates over time, decomposition alters the biochemical characteristics of solid peat down the soil profile, such as preferential preservation of lignin, a loss of lipids, and consistent carbohydrate content. D) Alternative scenarios are shown for gases produced within the peat soil exhibit C isotopic signatures that reflect the dominant source material, or a combination of both sources. Both organic inputs can contribute to gas production—either from a single source (top orange box and bottom orange box) or a mix of both (middle orange box). E) The results of this study indicate that the top scenario is most likely for these sites, with younger DOC fueling belowground respiration and methanogenesis, as illustrated in the red box.

## 2 Methods

 **2.1 Field Site Description**

The Bocas del Toro Province on the Caribbean coast of Panama is home to San San Pond Sak, an internationally recognized Ramsar site (#611), which highlights the global significance of this wetland. This site includes the 80 km² Changuinola peat deposit, an ombrotrophic domed peatland located southeast of the Changuinola River (Fig. 2). Located 10 km east from the peatland is the town of Bocas del Toro, Isla Colon, where the average annual rainfall and temperature are 4000 mm and 30°C respectively (Isla Colon, STRI Environmental Monitoring Station). There is continuous rainfall throughout the year with no pronounced dry season, although there are two distinct periods of lower rainfall (February–April and September–October). The water table was consistently at the surface of the peatland throughout the sampling period, but has been reported to fluctuate from 20cm above to 40cm below the peat surface during high or low rainfall (Hoyos-Santillan, 2014). Mean peat temperature 10 cm below the surface is 25 °C and shows little intra-annual variation (Wright et al., 2011). The oldest deposits in the peatland are in the centre of the dome, are estimated to have been formed 4000–4500 years ago, and are roughly 8 m deep (Phillips et al., 1997).

The Changuinola peat deposit developed from *Raphia taedigera* palm swamp, unlike southeast Asia coastal peatlands that begin as sediment trapping mangrove stands (Anderson and Muller, 1975; Phillips et al., 1997). The vegetation communities that formed the Changuinola peat deposits have shifted spatially over time, reflecting variations in environmental conditions, and resulting in spatial heterogeneities in C inputs across the peatland (Cohen et al., 1989; Phillips and Bustin, 1996). At present, there are seven distinct phasic plant communities that form concentric rings within the peat dome. From the periphery and moving to the interior they are as follows: (i) *Rhizophora mangle* mangrove swamp, (ii) mixed back mangrove swamp, (iii) *Raphia taedigera* palm swamp, (iv) mixed forest swamp, (v) stunted *Campnosperma panamensis* forest swamp, (vi) sawgrass/stunted forest swamp and (vii) *Myrica-Cyrilla* bog-plain (Phillips et al., 1997). Previous work showed that nutrient content in the peat was generally higher near the edge (1200 µg-phosphorus (P)g$^{-1}$, 27mg-nitrogen (N)g$^{-1}$) and lower in the interior of the peatland (377 µg-Pg$^{-1}$, 22mg-Ng$^{-1}$) (Sjögersten et al., 2011; Troxler, 2007; Troxler et al., 2012).

**Commented [AH3]:** Use same units for both - cm or m?

For this study we selected sites in three of the representative plant communities, with dominant vegetation and nutrient patterns described previously. These include Outer (*Raphia taedigera* palm swamp), Intermediate (mixed forest swamp), and Inner (stunted *Campnosperma panamensis* forest swamp) peatland sites (Fig. 2). Previous studies conducted within the Changuinola deposit have reported differences in peat properties, root exudate characteristics, and *ex situ* experimental response in lab studies tied to vegetation community (Girkin et al., 2018b, 2019; Sjögersten et al., 2011; Upton et al., 2018; Wright et al., 2013). Previously reported surface (<30 cm) $CO_2$ flux rates for the outer and inner sites used here varied from 320-500 mg $CO_2$ m$^{-2}$ hr$^{-1}$ with no significant variation between sites (Wright et al., 2011), and subsurface peat (below 30 cm) appeared to have similar carbohydrate to aromatic C ratios at the surface (Upton et al., 2018).
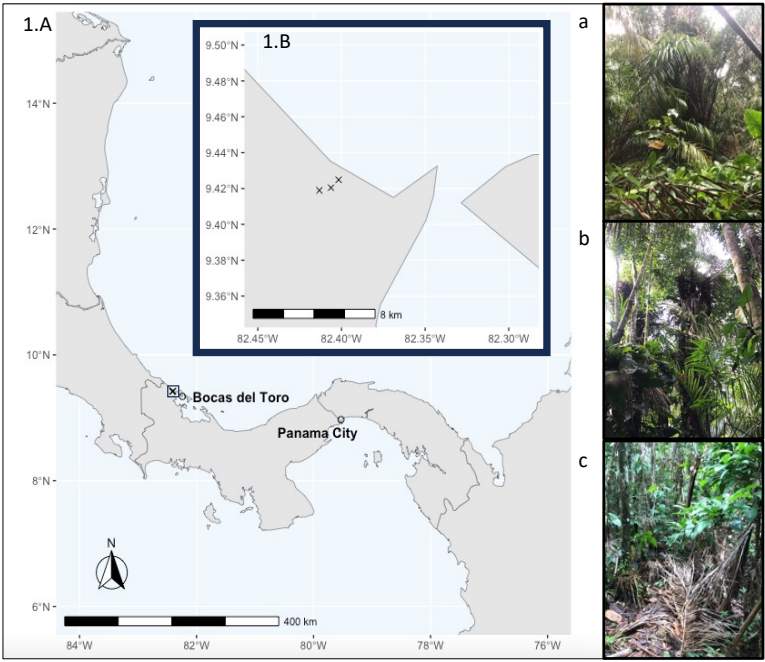
**Figure 2: Map of sites included in this study from the Changuinola peat deposit. A.** Location of study site identified by square in relation to the city of Bocas Del Toro and Panama City. **B.** Inset showing the location of the sites along the transect. The sites follow a vegetation gradient with a) the outer site closest to the channel *Raphia taedigera* palm swamp b) the intermediate site mixed forest swamp and c) the inner site closest to the centre of the peatland composed of stunted *Campnosperma panamensis* forest swamp. The nutrient gradient decreases from outer site to inner site.

## 2.2 Sample Collection

195     Bulk peat, pore water samples, and greenhouse gases ($CO_2$ and $CH_4$) were collected in October of 2019. We sampled from 30 cm to basal depths that were identified by a marine clay boundary at the base of the peat, and did not sample surface samples (0–30 cm) that might have stronger surface vegetation influence on peat chemistry compared to deeper layers that are further along in the decomposition process (Barreto and Lindo, 2020). This study aimed to compare bulk peat and pore water components of deep peat with gas produced at the same depth, and for that reason only those deeper samples were collected.

200     Peat cores were collected using a 5.2 cm diameter and 51 cm long peat sampler (Eijkelkamp, Product code 04.09). Bulk peat, pore water samples, and greenhouse gases ($CO_2$ and $CH_4$) were collected in October of 2019 from depths of $30 \pm 5$ and $60 \pm 5$ cm, as well as $100 \pm 5$, $200 \pm 5$, $300 \pm 5$, and $400 \pm 5$ cm depending on total peat depth at each site. Porewater was collected using a peristaltic pump with Teflon tubing from 1.25 cm diameter PVC pipe piezometers to measure DOC from the same depths as the peat collection. Porewater was filtered with 45 um particle retention using plastic syringes fitted with stopcocks and filters and deposited into 50 ml falcon tubes for transport. Following collection, peat cores were subsampled to coordinate

205     with gas well depths and sealed in plastic bags to avoid oxidation during transport to the Smithsonian Tropical Research Institute soils lab in Panama City, Panama.

        Diffusion gas wells were deployed at the intermediate and outer site at the same depths as pore water and peat collection to ensure robust comparison between the two source materials (bulk peat and DOC) and respiration products. There

210     was insufficient time to include the inner site in gas collection at time of sampling. These diffusion wells consisted of PVC pipe with mesh coverings positioned within the peat to allow water to be sampled from the desired depth without contamination of bulk peat or water pulled from other depths. Water was taken from the desired depth using a peristaltic pump and cycled into a 1L glass container. The headspace within the glass container was allowed to equilibrate over several hours while the water was pumped through the container at a rate of 1.5–1.8 L/min. Air samples from the equilibrated headspace were taken

215     using a syringe fitted with a stopcock and needle and deposited into evacuated 125 ml serum bottles fitted with heavy butyl rubber septa.

## 2.3 Elemental and Isotopic Analyses

        Elemental composition of solid homogenized airdried peat was analysed using an elemental analyser 205 (CHNOS) coupled to an IsoPrime 100 isotope ratio mass spectrometer at the Center for Stable Isotope Biogeochemistry (CSIB) 206 at

220     the University of California, Berkeley. This analysis produced measurements for percent C and N content, $^{13}C$, and $^{15}N$. The ash content of bulk peat was determined by ignition of aliquots ($\sim$1.0 g) at 460°C for 5 hr.

        Sample preparation and analysis for $\Delta$ $^{14}C$ was completed at the Center for Accelerator Mass Spectrometry (CAMS) at Lawrence Livermore National Laboratory. To ensure that peat samples were handled appropriately for both biogeochemistry and chronology, following homogenization with a ball and mill grinder we measured two subsamples; one that underwent

225     acid-base-acid (ABA) pre-treatment to remove possible interfering carbonates and modern C derived humic acids, and a second

with no pre-treatment (Norris et al., 2020). Samples were immersed in 1N hydrochloric acid (HCl) to remove carbohydrates. Humic acids were then removed from the sample with 0.25M sodium hydroxide (NaOH) and treated with a 1N HCL immersion before they were rinsed with deionized water until neutral. The pre-treated samples were then placed on a heating block until dried. The two sets of peat samples had identical $\Delta^{14}$C results and the no pre-treatment values were used in this study (Table A1). The porewater DOC samples were acidified with 1N HCl at 70 ∘C to remove dissolved inorganic C and freeze dried. Both sets of peat samples and the residual DOC were loaded into quartz tubes with excess CuO and combusted at 900∘C to ensure complete combustion to $CO_2$.

Gas samples for $CH_4$ and $CO_2$ were extracted following the protocol outlined by McNicol et al (2020). For $^{14}CO_2$ samples, a series of cryogenic traps were used to purify and isolate the $CO_2$. For $^{14}CH_4$ samples, the mixed composition field samples were cryogenically purified to remove water and $CO_2$, and the remaining $CH_4$ was converted to $CO_2$ by combustion (Petrenko et al., 2008). Resulting $CO_2$ from samples was split to measure both a $\delta^{13}$C and $\Delta^{14}$C. Extracted $CO_2$ and $CH_4$ were analysed for $\Delta^{14}$C and $\delta^{13}$C when possible, but some sample masses were too small for both analyses (minimum 20 ug C needed for $\Delta^{14}$C analysis and for the purpose of this study, we prioritized measurements for $\Delta^{14}$C). The $\delta^{13}$C values were analysed at the Stable Isotope Geosciences Facility at Texas 210 A&M University on a Thermo Scientific MAT 253 Dual Inlet Stable Isotope Ratio Mass Spectrometer. To obtain a $\Delta^{14}$C measurement, the $CO_2$ was reduced to graphite onto Fe powder in the presence of H2 (Vogel et al., 1984) and analysed on the HVEC 10 MV Model FN Tandem Van de Graaff Accelerator or the NEC 1 MV Pelletron Tandem Accelerator at CAMS (Broek et al., 2021). $\Delta^{14}$C values are reported as $\Delta^{14}$C (‰) corrected to the year of measurement (2019) and for mass-dependent fractionation using $\delta^{13}$C values, and age is reported in years before present (yBP) within two standard deviations using the Libby half-life of 5568 years following the conventions outlined by Stuiver and Polach, 1977. Age-depth models were generated for each site in R v.4.2.2 (The R Foundation for Statistical Computing, 2022) using the "rbacon" package v2.3.9.1. BACON (Bayesian accumulation), is based on Bayesian theory, and simulates the sediment deposition process while accounting for both variable deposition rates and spatial autocorrelation of deposition from one layer to another within the core. Long-term peat accumulation rates were estimated by fitting linear regressions to age-depth model outputs. The calibrated ages showed timing of peat development and accumulation between the three sites, and the conventional radiocarbon values were used to compare and identify the sources of material used to generate $CO_2$ and $CH_4$ at depth.

Differences in stable isotopic ($\delta^{13}$C) composition between $\delta^{13}CO_2$ and $\delta^{13}CH_4$ can identify the dominant pathway that produces methane, because hydrogenotrophic methanogenesis fractionate against heavy C isotopes more than acetoclastic methanogenesis (Wilson et al., 2016). Based on the measured stable carbon isotope signatures of $CH_4$ ($\delta^{13}$C-$CH_4$) and $CO_2$ ($\delta^{13}$C-$CO_2$) in dissolved gas in peat pore water, we calculated the apparent carbon isotope fractionation ($\alpha_{app}$) for this methanogenic process according to formula: $\alpha = (\delta^{13}CO_2 + 1000)/ (\delta^{13}CH_4 + 1000)$. Values of $\alpha_{app} = [(\delta^{13}CO_2 + 1000)/ (\delta^{13}CH_4 +1000)])$ that are greater than 1.065 are characteristic of environments dominated by hydrogenotrophic methanogenesis, while values lower than 1.055 are characteristic of environments dominated by acetoclastic methanogenesis (Zhang et al., 2019).

### 2.4 $^{13}$C-NMR Spectroscopy and Mixing Model

Solid State $^{13}$C NMR spectra of untreated peat samples were obtained at the Pacific Northwest National Laboratory in Washington state at the Environmental Molecular Science Laboratory facility using cross-polarization under magic angle spinning conditions (CP/MAS) with a Varian Direct Drive NMR spectrometer equipped with a Varian 4-mm probe. These bulk peat samples were free of charcoal. Approximately 30 mg of peat were packed in 4 mm zirconia rotors sealed with Kel-F caps. The CP spectra were acquired after 14k scans with a MAS rate of 14 kHz resulting in no interference from sidebands as they were outside the range of the spectrum, and a ramp-CP contact time on proton of 1 ms and a 1 or 2 s recycle delay depending on the sample with 62.5 kHz tppm proton decoupling (Aliev, 2020). The one-dimensional 1H NMR spectra of all samples were processed and analysed relative to the external standard adamantine. All spectra were corrected against a KBr background, and signals arising from C in the NMR probe and rotor were accounted for by subtracting the spectra of an empty rotor from the sample. Spectra were digitally processed with exponential apodization (100 Hz line broadening with the first point set to 0.50), phase correction, and baseline correction using a Bernstein polynomial fit with Mnova software (v. 14.3.3; Mestrelab Research). Peak areas were integrated within seven chemical shift regions for input to the molecular mixing model corresponding to: alkyl C (0–45 ppm), N-alkyl/methoxyl C (45–60 ppm), O-alkyl C (60–95 ppm), di-O-alkyl (95–110), aromatic C (110–145 ppm), phenolic C (145–165 ppm), and carboxyl C (165–215 ppm).

We used a mixing model which incorporates six components to describe the molecular composition of samples based on $^{13}$C NMR outputs (Baldock et al., 2004). This peatland soil has no visual evidence of char, so that component was removed from the model. The five remaining components (carbohydrate, protein, lipid, lignin, and carbonyl) have each been assigned a discrete percent of different regions of the $^{13}$C NMR signal intensity based on knowledge of molar elemental contents and C content of terrestrial soil ecosystems. The measured C:N ratio of each sample was used to constrain the protein concentration of each $^{13}$C NMR spectrum in the molecular mixing model. The optimisation process of the molecular mixing model compares fits for all five biomolecules to models eliminating one, two, and three components; in all cases the model fit was best when all five components were included in the model (sum of squares of deviation < 6%). The mixing model outputs are available in Table A2.

### 2.6 Statistics

We assessed our data at two scales: 1) among-site comparisons of the three sites, considering overall differences in peat characteristics and isotopic signatures and 2) peatland-wide patterns in soil profile characteristics and relationships among peat chemistry and isotopic signatures. Relationships between peat physical properties (C and N concentrations, C:N, $^{13}$C,$^{15}$N, and radiocarbon) and the five biomolecules identified with the molecular mixing model were assessed using Pearson correlation analysis. We also conducted separate analyses of the $^{13}$C-NMR data using raw data for spectral regions. The three sites were pooled to get peatland scale relationships between the peat physical properties and the five biomolecules versus depth. Due to the limited size of this dataset, the spearman method was used to measure covariance and the coefficients are

reported in the full correlation matrix results, including r² values and significance, in supplementary materials (Fig. A3 & A4).

300 We assessed differences among the three sites using Principal Component Analysis (PCA) based on all factors included in the correlation matrices (all peat physical properties, chemistry, and isotopes for each site). Significant trends in biomolecule abundance across depth were identified by linear regression. To identify differences between mean radiocarbon values of the sources and respiration products we utilized two-sample t-tests. Bulk peat and gas products were determined by Welch two-sample t-test to account for lack of homogeneity of variance, and differences between mean radiocarbon values of DOC and

305 gas products were assessed by student two sample t-test. All relationships explored were considered significant at the 0.1 alpha level. Statistical analyses were conducted in R v.4.2.2 (The R Foundation for Statistical Computing, 2022). Reported means in the text are shown with standard errors in parentheses.

## 3 Results

### 3.1 Isotopic composition of source material and respiration products

310 Across all sites and depths, dissolved $CH_4$ and $CO_2$ were relatively modern, ^{14}C-enriched relative to peat, and had similar $\Delta$[14]C values to DOC, indicating the use of DOC as a preferential substrate over solid peat for microbial respiration (Fig 3). Overall, the respiration products had statistically similar values to the DOC (t(23)=0.534 p= 0.60) compared to the bulk peat (t(16)=|8.67|, p= <0.05) (Table S3). The radiocarbon values for the bulk peat are consistent with constant accumulation over time. The calibrated basal ages for outer, intermediate, and inner sites were 1215 ± 35, 1060 ± 30, and 1750 ± 35 yrBP

315 respectively.
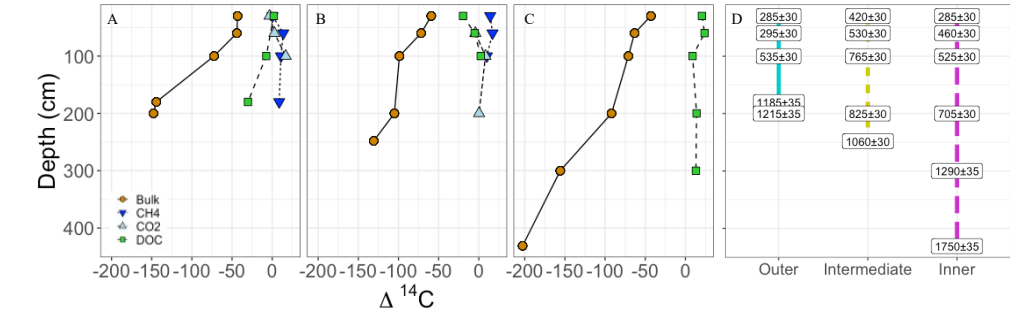
**Figure 3. Isotopic composition of respiration products and substrates.** Bulk peat, DOC, and respiration products ($CH_4$ = methane, $CO_2$ = carbon dioxide) plotted by depth across all three sites; **A)** Outer, **B)** Intermediate and **C)** Inner. Brown circles and solid lines represent bulk peat and green squares with dashed lines represent DOC; these are the two measured sources available for gas production. The gas products are denoted by inverted dark blue triangles and dotted lines for methane, and the light blue triangles and dashed lines for dissolved carbon dioxide. Note the age difference between solid peat and all DOC and gas values; this offset indicates that gas production is driven by modern DOC throughout the peat profile. **D.** Calibrated ages for all bulk peat measured in yBP within two standard deviations for the outer, intermediate, and inner sites denoted by solid blue, dashed yellow, and dashed pink respectively.

### 3.2 Peat Properties and Chemistry

The percent OC across the sites was consistently 40–55% down to basal depths, which had lower OC contents and higher ash content, reflecting the influence of underlying mineral sediments (Fig. 4). The negative correlation between both OC and N concentrations with depth was not significant, however the negative correlations between ash content and depth (r (16) = - 0.62, p≤0.1) and age and depth (r (16) = - 0.93, p≤0.1, Fig. 4) were strongly significant (Fig. A3). Bulk peat stable isotopes, $\delta^{13}$C and $\delta^{15}$N, showed no strong relationship with depth or site. Linear slopes across the age-depth profiles suggested consistent peat accumulation rates across the peatland over time (Fig. 4f). Estimates of long-term peat accumulation rates were calculated using the calibrated ages, and were 0.192 cm yr$^{-1}$, 0.473 cm yr$^{-1}$, and 0.275 cm yr$^{-1}$ for the outer, intermediate, and inner sites respectfully.
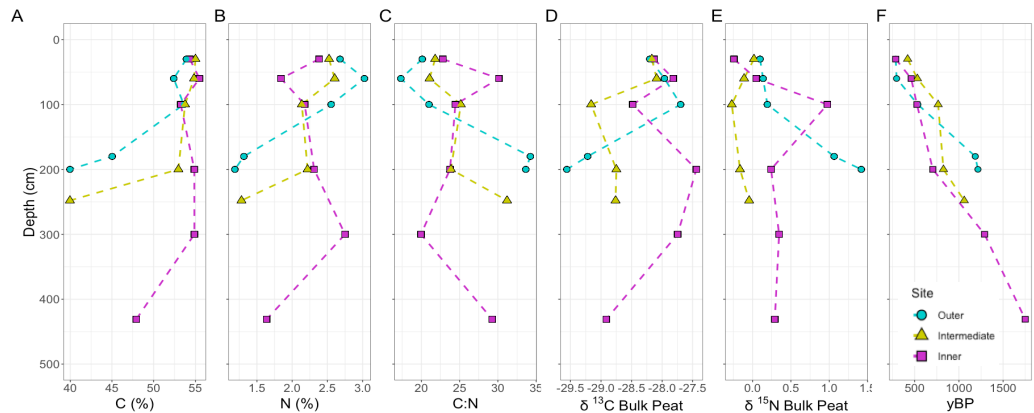
**Figure 4. Bulk Peat Properties and Characteristics.** Depth profiles for A. percent carbon, B. percent nitrogen, C. the ratio of carbon to nitrogen, D. stable carbon isotope, E. stable nitrogen isotope, and E. calibrated age for layers measured for the three sites. Sites are indicated by colour and shape with blue circles indicating the outer site, yellow triangles the intermediate site, and pink squares the inner site.

2% ± 2 carbonyl-C respectively (Fig 6. A&C). Overall, the organic chemistry of peat was very similar across the sites explored here, and the main patterns that emerged were trends with depth.
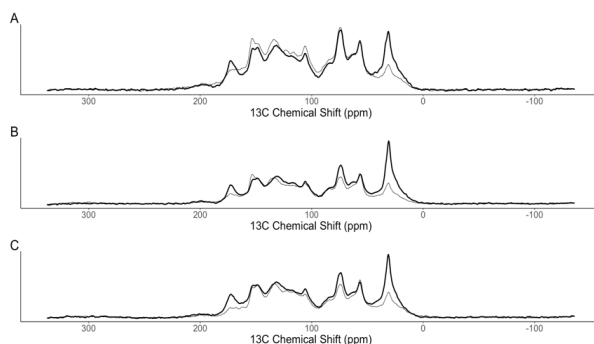
**Figure 5. Example 13C NMR spectra.** Bulk peat layers sampled from the A. outer, B. intermediate, and C. inner sites showing differences between the shallow (bold) and basal (thin) depths with stacked spectra; the complete spectra dataset can be found in additional data located in supplemental material. Spectra were digitally processed with Mnova software (v. 14.3.3; Mestrelab Research) with exponential apodization (100 Hz line broadening with the first point set to 0.50), phase correction, and baseline correction using a Bernstein polynomial fit.
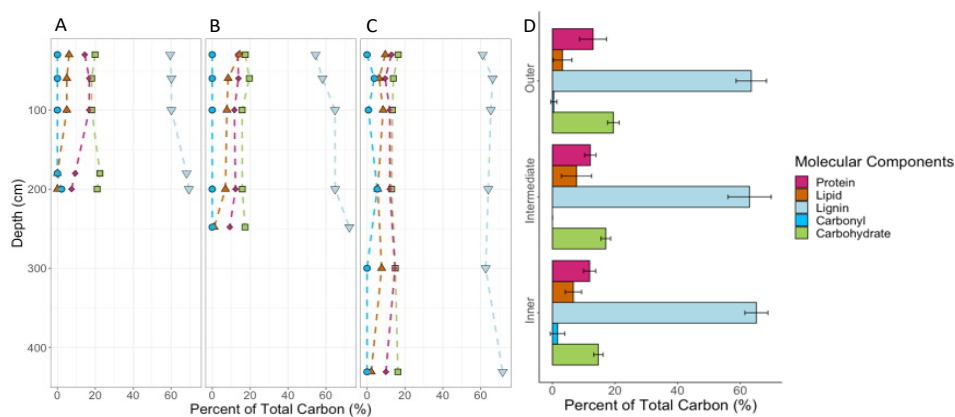
**Figure 6. Proportion of total organic C attributed to each molecular component across sites and depths.** Mixing model results showing little change in the five molecular components described by the model with depth for the **A)** outer site, **B)** intermediate site, and **C)** inner site. Colours and symbols represent the molecular components with proteins as pink diamonds, lipids as orange triangles, lignin as light blue inverted triangles, carbonyl as blue circles, and carbohydrates as green squares. **D)** Average proportion of total organic C attributed to each molecular component across sites with standard error.

We used PCA to explore differences in peat properties among the three sites. The scores and loadings of the first and second principal components accounted for the majority of variance (74%) with the first principal component accounting for 54.93% (Fig 7). Separation along the first principal component axis showed stratigraphic effects related to depth and peat accumulation over time, with strong separation between the 30 and 60 cm layers versus the underlying peat. The clustering of the 30 and 60 cm peat layers was primarily driven by OC and N concentration, age, ash content, and lipid, alkyl-C, and protein contributions to soil OC (Fig 7, Table A2). By contrast, the second principal component was mainly driven by site differences, with the inner site being relatively more distinct than the outer and intermediate sites while still showing some overlap (Fig 7). This separation appeared to be tied to the small amount of carbonyl present at this site (Fig 7, Table A2, Table A4).

**Figure 7. Scores and loadings from the PCA** for all peat properties and chemistry and depth for the outer (blue), intermediate (yellow), and inner (pink) sites. Depths have been indicated by shape with the top (30-60 cm) as circles, the bottom (>1 m) as triangles, and the three basal depths as squares (basal depths; Outer 200 cm, Intermediate 248 cm, and Inner 431cm). Combined PC1 and PC2 account for 74% of variance.

Deleted: C

Deleted: organic C

**3.3 Using δ¹³C to identify CH₄ Production Pathway**

The $\alpha_{app}$ values overlap between the outer and intermediate sites and averaged 1.078 (+/- 0.003) (Fig. 8). These data demonstrate no shift in $\alpha_{app}$ with depth throughout the peat profile. The $\alpha_{app}$ is consistent with hydrogenotrophic methanogenesis being the dominant production pathway across all depths measured at the outer and intermediate sites.
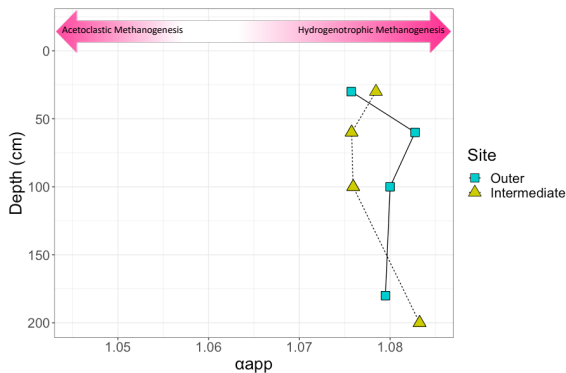
**Figure 8. Differences in stable C isotopic composition between DIC and CH₄.** Calculated estimates of apparent fractionation factor (αapp) across depth for gas collected from the outer (blue squares) and intermediate (green triangles) sites. The samples from the inner site did not have sufficient amounts of C for this analysis. Note the x-axis shows little variation in αapp between sites and soil layers; values of αapp higher than 1.065 is usually characteristic of environments dominated by hydrogenotrophic methanogenesis, while a value lower than 1.055 is characteristic of an environment dominated by acetoclastic methanogenesis (Corbett et al., 2013).

## 4. Discussion

### 4.1 Source

The Changuinola peat deposit is important as an internationally protected wetland and is an example of a pristine undisturbed functioning tropical peatland. This is supported by the age-depth profiles that showed continuous undisturbed peat accumulation over time, and similarities in OC and N concentrations and C:N ratios to other ombrotrophic peat domes across the tropics (Beilman et al., 2019; Dargie et al., 2017; Lähteenoja et al., 2012; Omar et al., 2022). This paper contributes a novel characterization of the organic components contributing to surface $CO_2$ and $CH_4$ fluxes (bulk peat, respiration products, peat chemical composition) to identify the dominant source of OC for a tropical peatland. Across all sites and depths, DOC exhibited enriched radiocarbon signatures compared to the bulk peat, indicating it is largely derived from recent photosynthate. This suggests that while the DOC originates from newer organic material, the solid peat becomes progressively older with depth, confirming that the peat found in deeper layers is indeed older. Most importantly, we demonstrate that while both of these

sources are available for utilization, the respiration products closely resemble, if not completely match, the DOC, indicating that DOC is currently the source of CO2 and CH4 in this peatland.

370  Similar behaviour has been reported in other tropical peatlands that preferentially use modern DOC as the source for microbial respiration ( Hoyt et al., 2020), while one site in Borneo reported respiration products from mixed sources (Hoyt, 2014). These contrasting results suggest either the Borneo peatland site is an exception to this behaviour or there is need to explore more tropical peatland sites to characterize source selection behaviour in the tropics. Our findings indicate that surface-derived DOC significantly influences gas production deep within the soil profile, potentially linked to the high lignin content typical of wood-dominated peatlands. At our sites, contrasting surface vegetation types—*Raphia taedigera* and mixed

375  hardwood—supply the organic matter for DOC. Enriched radiocarbon signatures in deeper DOC suggest that this organic carbon primarily originates from surface sources, emphasizing the critical role of DOC substrates throughout the peat profile. Even at greater depths, the influence of surface vegetation remains significant, underscoring the importance of surface-derived DOC for carbon dynamics in these ecosystems. Tropical peatlands with higher abundances of sedge or shrub species may exhibit different source selection preferences based on variations in DOC, root exudates, and peat composition (Girkin et al.,

380  2018a; Waldron et al., 2019).

**4.2 Peat Chemistry and Stabilization**

The dominant biomolecule making up this peat OC was lignin, which generally represented >60% of the OC in our samples. Despite the lack of a depth difference in the aromaticity index, we saw an accumulation of lignin with depth, indicating preferential preservation of this biomolecule and microbial discrimination against its decomposition through time.

385  This selective preservation of lignin has been reported for this wetland (Hoyos-Santillan et al., 2016) and other tropical peatlands (Gandois et al., 2014) previously, and supports a paradigm of selective preservation of aromatic compounds under anaerobic conditions. Coarse woody material from fallen trees, branches, and dead roots contribute a large yet relatively sporadic portion of OC inputs to tropical peat, in addition to the more constant inputs from leaf litter and fine root turnover (Hodgkins et al., 2018), and our data together with the previous studies indicate that this large-scale tree mortality and branch

390  shedding is crucial for peat OC accumulation. The waterlogged conditions in tropical peatlands can particularly reduce the decomposition of lignin by inhibiting ligninolytic microbes (Hoyos-Santillan et al., 2015; Thormann, 2006). There was little change in the carbohydrate portion of peat OC with depth, even though carbohydrates typically represent the most labile compounds in plant tissues for decomposition (Bader et al., 2018). This lack of change in carbohydrate abundance with depth below 30 cm may indicate consistent preservation of this molecule after any initial decomposition in the top 30 cm, and

395  contrasts with the preferential preservation of lignin. Interestingly, we see a significant decline in lipids with depth, even though other tropical and temperate forest studies have indicated preferential preservation of lipids in upland soils (Cusack et al., 2018; Jastrow et al., 2007; Wiesenberg et al., 2010). Our data suggest that under anaerobic conditions, lipids are decomposed more than other compounds, and/or microbial biomass production of lipids declines, or changes in carbon inputs over time. Taken together, our data support different decomposition rates and preservation processes of individual biomarkers

that contribute to the accumulation of OC within tropical peatlands. Specifically, there is evidence of varying rates of biomarker degradation related to the composition of the organic matter in these sites, suggesting that certain compounds are more resistant

420 to decomposition (Girkin et al., 2018a). Meanwhile, specific environmental conditions and microbial communities can also influence the preservation of these biomarkers, further supporting our findings that the interplay between biological origin and decomposition processes is critical for understanding OC dynamics in tropical peatlands (Hoyos-Santillan et al., 2016). Together, these studies reinforce the complexity of OC dynamics and the significance of individual biomarkers in shaping C storage within these ecosystems.

425    Our outer site is closest to the edge of the peatland in an area in the peatland that is dominated by *Raphia taedigera* palm swamp and with relatively high nutrient availability, while the intermediate site dominated by mixed forest swamp species, and the inner site closest to the centre of the peatland dominated by stunted *Campnosperma panamensis* forest and has relatively low nutrient availability (Phillips and Bustin, 1996; Sjögersten et al., 2011; Troxler, 2007). Despite these documented differences, we found strong similarity across sites in peat characteristics as well as the radiocarbon content of porewater DOC,

430 $CO_2$, and $CH_4$. Our results demonstrate that the peat at or below 2 m is relatively carbohydrate- and lignin-rich and potentially less decomposed than expected, making these soils vulnerable to rapid decomposition if exposed to aerobic conditions.

    Based on the $\Delta$ $^{14}$C and age of peat collected across these sites, the dome shape of the peatland has built up with older layers closer to the surface at the margins (Fig 9). This shape and accumulation pattern has been described and modelled across other tropical peat domes that have the similar ombrotrophic characteristics as Changuinola (Cobb et al., 2017, 2024). Our

435 results suggest age was not a driver of peat chemical characteristics or properties that describe decomposability, and that older peat that accumulated over 1000 years ago is closer to the surface at the margins and would be the first layers to experience aerobic conditions with changes in water table draw down or disturbance (Dommain et al., 2011).
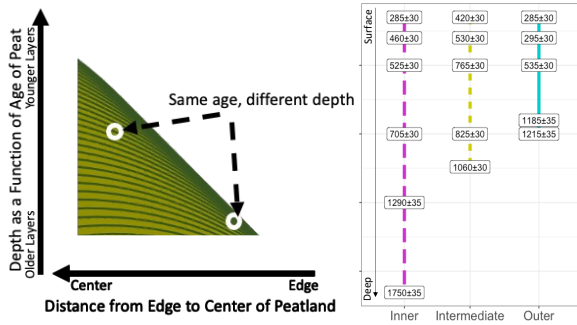
**Figure 9: Schematic of peatland shape and layer accumulation pattern based on peat layer age and depth from surface**. This concept was presented in model data from Cobb et al., 2017 and has been modified to create this schematic that is not to scale. Peat layers accumulate over time with the youngest layers at the surface and oldest layers at the base of the peat deposit. Based on this and ages collected from the sites within the Changuinola peat deposit, layers that correspond to the same age are located at different depths across the peat dome with older peat layers are closer to the surface at the margins.

**Using $\delta^{13}C$ to understand $CH_4$ Production**

Peat organic matter quality not only influences decomposition rates but also affects the pathway of $CH_4$ production (Holmes et al., 2015). When easily degradable inputs are decomposed, acetate is produced by fermentative bacteria, enhancing the role of acetoclastic methanogenesis (Mobilian and Craft, 2022). As labile material becomes depleted, the decomposition of more resistant compounds and the associated $CO_2$ production promote a shift toward hydrogenotrophic methanogenesis (Conrad, 2020). The high observed $\alpha_{app}$ (1.078 ± 0.003) within this study suggests that hydrogenotrophic methanogenesis is the primary $CH_4$ production pathway, with no evidence of depth-related variation. These findings align with Holmes et al. (2015), who reviewed fractionation factors across global peatlands.

While we cannot map the exact progression from plant material to $CH_4$, hydrogenotrophic methanogenesis depends on $CO_2$ availability for reduction to $CH_4$, with $CO_2$ from initial decomposition steps likely serving as a key source (Gruca-Rokosz and Koszelnik, 2018; Kotsyurbenko et al., 2004). This cooperative microbial interaction, where primary degraders supply necessary precursors (in this case, $CO_2$) for further metabolism, has been observed in soils and may regulate $CO_2$ release within this peatland (Chen et al., 2023; Li et al., 2021). Further investigation into the methanogen community structure and stratigraphy is needed to better understand the factors affecting net $CH_4$ flux from this wetland and to determine whether surface processes could alter $CH_4$ production pathways in the upper (0–30 cm) peat layer.

Although both northern and tropical peatlands may exhibit hydrogenotrophic methanogenesis as the dominant pathway, the $\delta^{13}C$-$CH_4$ signature differs widely due to variations in precursor $\delta^{13}C$-$CO_2$, influenced by temperature, microbial activity, organic matter composition, and decomposition processes (Holmes et al., 2015). In cold, highly anoxic northern peatlands, $\delta^{13}C$-$CO_2$ tends to be more depleted due to extensive carbon recycling in low temperatures and high water tables, which slows organic matter decomposition and allows for greater microbial processing that further depletes $\delta^{13}C$ (Rinne et al., 2022). In contrast, the warmer, more readily decomposable organic material in tropical peatlands results in less depleted $\delta^{13}C$-$CO_2$ values (Holmes et al., 2015). While this study does not imply that tropical peatlands function differently from temperate peatlands, these findings suggest that research in higher-latitude peatlands offers a basis to explore OC cycling in tropical peatlands. However, additional validation is needed to confirm that they operate similarly.

**Future Implications**

Tropical peatlands, such as the Changuinola peat deposit, represent critical carbon-rich ecosystems that play a substantial role in the global carbon cycle but face vulnerability under future climate scenarios. Our findings show that these peatlands currently rely heavily on surface-derived DOC to support deep peat respiration, produce $CH_4$ primarily through hydrogenotrophic methanogenesis, and continue to accumulate lignin-rich, carbon-dense peat under anaerobic conditions. However, this carbon storage mechanism is sensitive to shifts in climate, hydrology, and vegetation. Changes in precipitation patterns and increased evapotranspiration associated with climate change could disrupt the connectivity between surface and

deep peat layers, altering DOC transport and potentially increasing the exposure of preserved peat to aerobic conditions. The predominance of lignin, resistant under anoxic conditions, raises questions about its vulnerability when exposed to oxygen. If peatlands dry out, the preserved OC could rapidly decompose, shifting the ecosystem from a sink to a potential carbon source, with significant greenhouse gas release (Kettridge et al., 2015; Ofiti et al., 2023).

Our study underscores the need for further research on the resilience of tropical peatlands under changing environmental conditions. Key areas for future work include examining how shifts in vegetation and surface inputs could influence OC dynamics and gas production. Variations in plant community composition and changes in nutrient status may affect DOC quality and quantity, potentially altering the balance between acetoclastic and hydrogenotrophic methanogenesis pathways. Additionally, further investigation into the microbial communities driving peat decomposition and $CH_4$ production could yield insights into how these processes may shift with changing environmental factors.

Comparative studies between high-latitude and tropical peatlands highlight the unique characteristics of tropical systems, which are subject to faster biomass production and decomposition rates in warmer climates. Unlike high-latitude peatlands, which accumulate OC slowly over millennia, tropical peatlands maintain a more dynamic OC balance. This difference suggests that tropical peatlands may be particularly vulnerable to rapid changes in hydrology and land use. Understanding how such factors interact to influence peat accumulation, organic matter preservation, and greenhouse gas flux is essential for assessing the stability of tropical peatlands in a warming world.

To fully realize the climate mitigation potential of tropical peatlands, future studies must address how these ecosystems respond to both gradual and abrupt environmental changes. The development of long-term conservation and restoration strategies will depend on our ability to anticipate the impacts of altered hydrology and vegetation composition on peatland OC storage. Continued research into these processes is vital for informing global climate policies and ensuring the preservation of these irreplaceable OC reservoirs.

## Appendix A

550

Table A1: **Radiocarbon results for both untreated (No Acid-Base-Acid) and treated (Acid-Base-Acid) sets of peat samples**. Radiocarbon concentration is expressed as $\Delta^{14}$C within two standard deviations.

| Site | Depth | $\Delta^{14}$C (No ABA) | ± | $\Delta^{14}$C (ABA) | ± |
|---|---|---|---|---|---|
| Outer | 100 | -72.4 | 3.1 | -77.5 | 4.0 |
| | 180 | -147.8 | 3.2 | -157.6 | 3.6 |
| | 200 | -144.3 | 3.2 | -157.8 | 3.6 |
| | 30 | -43.1 | 3.4 | -54.9 | 4.1 |
| | 60 | -44.0 | 3.4 | -54.2 | 4.1 |
| Intermediate | 30 | -59.2 | 3.4 | -59.9 | 4.0 |
| | 60 | -71.8 | 3.3 | -70.2 | 4.0 |
| | 100 | -98.8 | 3.3 | -107.5 | 3.8 |
| | 200 | -105.1 | 3.2 | -110.8 | 3.8 |
| | 248 | -130.8 | 3.2 | -141.0 | 3.7 |
| Inner | 30 | -42.9 | 3.3 | -45.6 | 4.1 |
| | 60 | -63.3 | 3.3 | -68.5 | 4.0 |
| | 100 | -71.0 | 3.2 | -75.9 | 4.0 |
| | 200 | -92.0 | 3.3 | -93.6 | 3.9 |
| | 300 | -155.8 | 3.2 | -155.2 | 3.6 |
| | 431 | -202.7 | 3.1 | -203.1 | 3.4 |

555

560

Table A2: **Mixing model outputs for all depths sampled from the three sites.** Molecular component proportion of total C measured via ^{13}CNMR described by the mixing model output as weighted percent (Wt%) developed by Baldock et al., 2004, %C measured from bulk peat combustion via elemental analyzer.

| Site | Depth (cm) | Molecular Component | Wt% | %C |
|------|------------|---------------------|------|-------|
| Inner | 30 | Carbohydrate | 16.5 | 54.33 |
| Inner | 30 | Protein | 12.9 | 54.33 |
| Inner | 30 | Lignin | 61.0 | 54.33 |
| Inner | 30 | Lipid | 9.6 | 54.33 |
| Inner | 30 | Carbonyl | 0.0 | 54.33 |
| Inner | 60 | Carbohydrate | 13.9 | 55.49 |
| Inner | 60 | Protein | 9.6 | 55.49 |
| Inner | 60 | Lignin | 66.3 | 55.49 |
| Inner | 60 | Lipid | 6.4 | 55.49 |
| Inner | 60 | Carbonyl | 3.8 | 55.49 |
| Inner | 100 | Carbohydrate | 13.4 | 53.24 |
| Inner | 100 | Protein | 12.1 | 53.24 |
| Inner | 100 | Lignin | 65.3 | 53.24 |
| Inner | 100 | Lipid | 8.5 | 53.24 |
| Inner | 100 | Carbonyl | 0.7 | 53.24 |
| Inner | 200 | Carbohydrate | 13.0 | 54.87 |
| Inner | 200 | Protein | 12.1 | 54.87 |
| Inner | 200 | Lignin | 64.0 | 54.87 |
| Inner | 200 | Lipid | 5.7 | 54.87 |
| Inner | 200 | Carbonyl | 5.3 | 54.87 |
| Inner | 300 | Carbohydrate | 14.9 | 54.88 |
| Inner | 300 | Protein | 14.8 | 54.88 |
| Inner | 300 | Lignin | 62.6 | 54.88 |
| Inner | 300 | Lipid | 7.7 | 54.88 |

| Inner | 300 | Carbonyl | 0.0 | 54.88 |
|---|---|---|---|---|
| Inner | 431 | Carbohydrate | 16.3 | 47.91 |
| Inner | 431 | Protein | 9.9 | 47.91 |
| Inner | 431 | Lignin | 71.6 | 47.91 |
| Inner | 431 | Lipid | 2.2 | 47.91 |
| Inner | 431 | Carbonyl | 0.0 | 47.91 |
| Intermediate | 30 | Carbohydrate | 17.4 | 55.01 |
| Intermediate | 30 | Protein | 13.5 | 55.01 |
| Intermediate | 30 | Lignin | 54.5 | 55.01 |
| Intermediate | 30 | Lipid | 14.5 | 55.01 |
| Intermediate | 30 | Carbonyl | 0.0 | 55.01 |
| Intermediate | 60 | Carbohydrate | 19.6 | 54.84 |
| Intermediate | 60 | Protein | 13.8 | 54.84 |
| Intermediate | 60 | Lignin | 58.2 | 54.84 |
| Intermediate | 60 | Lipid | 8.4 | 54.84 |
| Intermediate | 60 | Carbonyl | 0.0 | 54.84 |
| Intermediate | 100 | Carbohydrate | 15.8 | 53.76 |
| Intermediate | 100 | Protein | 11.7 | 53.76 |
| Intermediate | 100 | Lignin | 64.8 | 53.76 |
| Intermediate | 100 | Lipid | 7.7 | 53.76 |
| Intermediate | 100 | Carbonyl | 0.0 | 53.76 |
| Intermediate | 200 | Carbohydrate | 15.9 | 52.96 |
| Intermediate | 200 | Protein | 12.3 | 52.96 |
| Intermediate | 200 | Lignin | 64.9 | 52.96 |
| Intermediate | 200 | Lipid | 7.0 | 52.96 |
| Intermediate | 200 | Carbonyl | 0.0 | 52.96 |
| Intermediate | 248 | Carbohydrate | 17.3 | 39.96 |

| | | | | |
|---|---|---|---|---|
| Intermediate | 248 | Protein | 9.3 | 39.96 |
| Intermediate | 248 | Lignin | 72.4 | 39.96 |
| Intermediate | 248 | Lipid | 1.0 | 39.96 |
| Intermediate | 248 | Carbonyl | 0.0 | 39.96 |
| Outer | 30 | Carbohydrate | 19.9 | 53.92 |
| Outer | 30 | Protein | 14.4 | 53.92 |
| Outer | 30 | Lignin | 59.5 | 53.92 |
| Outer | 30 | Lipid | 6.2 | 53.92 |
| Outer | 30 | Carbonyl | 0.0 | 53.92 |
| Outer | 60 | Carbohydrate | 18.1 | 52.40 |
| Outer | 60 | Protein | 16.8 | 52.40 |
| Outer | 60 | Lignin | 60.2 | 52.40 |
| Outer | 60 | Lipid | 5.0 | 52.40 |
| Outer | 60 | Carbonyl | 0.0 | 52.40 |
| Outer | 100 | Carbohydrate | 18.1 | 53.60 |
| Outer | 100 | Protein | 16.8 | 53.60 |
| Outer | 100 | Lignin | 60.2 | 53.60 |
| Outer | 100 | Lipid | 5.0 | 53.60 |
| Outer | 100 | Carbonyl | 0.0 | 53.60 |
| Outer | 180 | Carbohydrate | 22.4 | 39.96 |
| Outer | 180 | Protein | 9.4 | 39.96 |
| Outer | 180 | Lignin | 68.2 | 39.96 |
| Outer | 180 | Lipid | 0.0 | 39.96 |
| Outer | 180 | Carbonyl | 0.0 | 39.96 |
| Outer | 200 | Carbohydrate | 21.0 | 45.03 |
| Outer | 200 | Protein | 7.5 | 45.03 |
| Outer | 200 | Lignin | 69.4 | 45.03 |

| Outer | 200 | Lipid | 0.0 | 45.03 |
| Outer | 200 | Carbonyl | 2.2 | 45.03 |

565
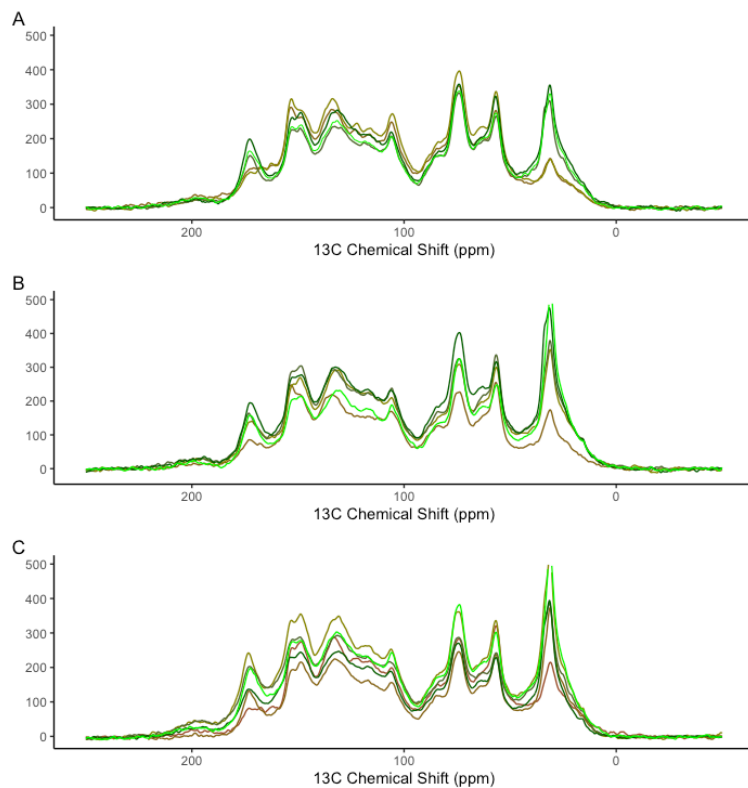
**Fig A2: Stacked overlay of depth profiles of ¹³C NMR spectra of the A) Outer, B) Intermediate, and C) Inner site. Colors increase in darkness representing an increase in depth with light green being the 30cm material and dark brown being the basal material. Spectra were digitally processed with Mnova software (v. 14.3.3; Mestrelab Research) with exponential apodization (100 Hz line broadening with the first point set to 0.50), phase correction, and baseline correction using a Bernstein polynomial fit. Peak areas were integrated corresponding to; alkyl C (0–45 ppm), N-alkyl/methoxyl C (45–60 ppm), O-alkyl C (60–95 ppm), di-O-alkyl (95–110), aromatic C (110–145 ppm), phenolic C (145-165 ppm), and carboxyl C (165–215 ppm).**

570

Fig A2
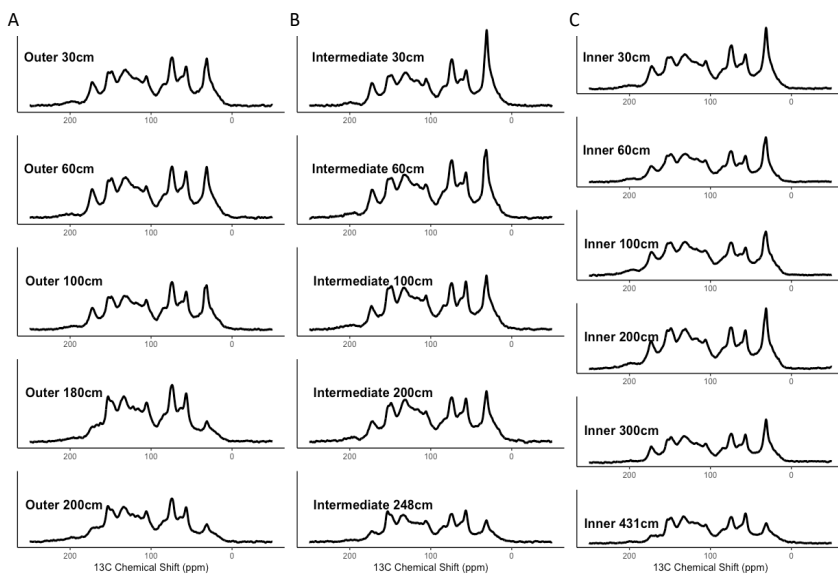
Fig A3: Depth profiles of $^{13}$C NMR spectra for the A) Outer, B) Intermediate, and C) Inner sites. Spectra were digitally processed with Mnova software (v. 14.3.3; Mestrelab Research) with exponential apodization (100 Hz line broadening with the first point set to 0.50), phase correction, and baseline correction using a Bernstein polynomial fit. Peak areas were integrated corresponding to; alkyl C (0–45 ppm), N-alkyl/methoxyl C (45–60 ppm), O-alkyl C (60–95 ppm), di-O-alkyl (95–110), aromatic C (110–145 ppm), phenolic C (145-165 ppm), and carboxyl C (165–215 ppm). The y-axis has been scaled equally across all plots to visually compare changes in peak heights and area across depth, however the additional depths at the Inner site need to be considered when comparing across sites.

575

580

**Table A3: Results from two-sample t-tests** comparing bulk peat radiocarbon vaues versus respiration product radiocarbon
585   values, and DOC radiocarbon values versus respiration product radiocarbon values.

|  | Sample Type | Mean | t-value | df | p-value |
|---|---|---|---|---|---|
| Pair 1 | Bulk Peat | -96.5625 | -8.6657 | 15.974 | 1.96E-07 |
|  | Gases ($CH_4$, $CO_2$) | 7.95 |  |  |  |
| Pair 2 | DOC | 2.027273 | 0.53811 | 23 | 0.5957 |
|  | Gases ($CH_4$, $CO_2$) | -3.878571 |  |  |  |

Fig A3

590
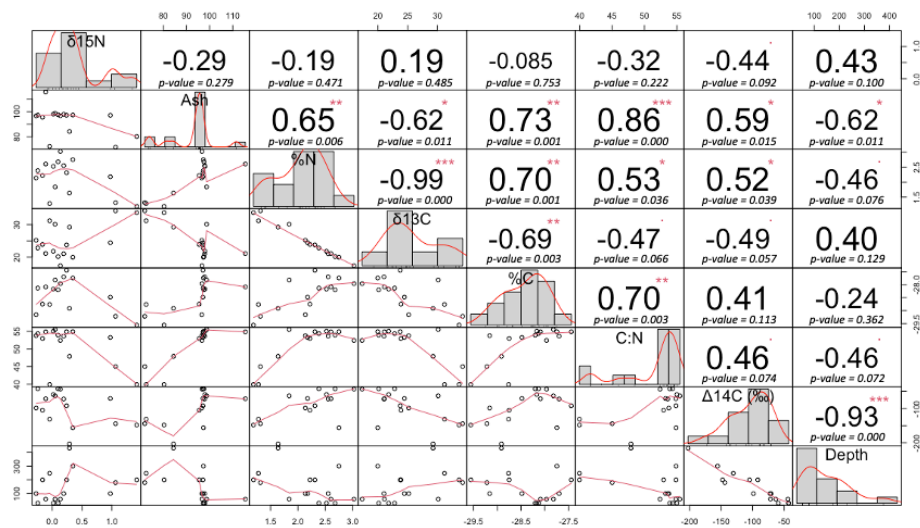
**Fig A3: Correlation matrix for peat physical properties and depth. The numbers represent the value of the correlation coefficient (r) plus the result of the cor.test as stars. On the bottom of the matrix are the bivariate scatterplots with a fitted line. Significand codes: 0 '***' 0.001 '**' 0.01 '*' 0.1 ' '.**

Fig A4
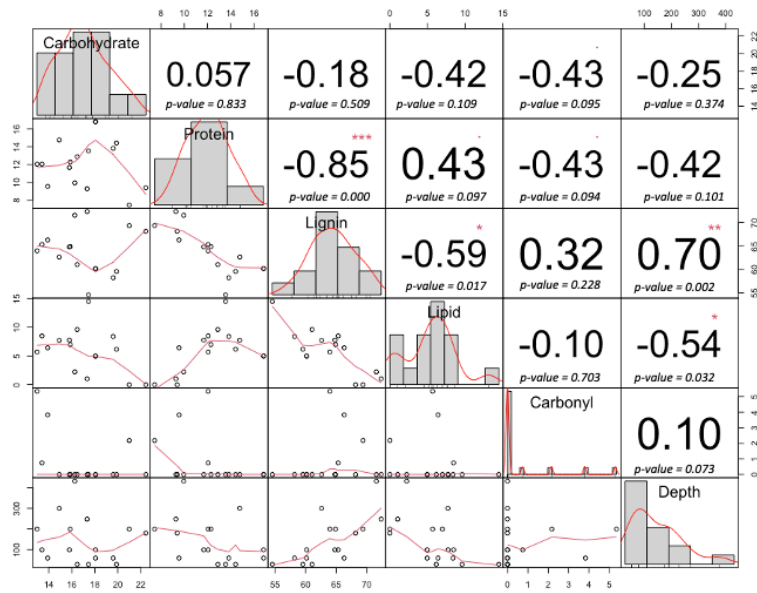
**Fig A4: Correlation matrix for peat molecular components and depth. The numbers represent the value of the correlation (r²) plus the result of the cor.test as stars. On the bottom of the matrix are the bivariate scatterplots with a fitted line. Significand codes:  0 '***' 0.001 '**' 0.01 '*' 0.1 ''.**

595

**Table A4**: PCA eigenvalues and loadings for PC1 and PC2.

| | PC1 | PC2 |
|---|---|---|
| **Eigenvalues** | **3.314e+00** | **1.941e+00** |
| *Variable* | | |
| $\delta^{15}N$ | -0.186 | 0.039 |
| Ash | -0.386 | -0.077 |
| %N | 0.274 | -0.109 |
| $\delta^{13}C$ | 0.230 | 0.165 |
| %C | 0.275 | 0.091 |
| C:N | -0.266 | 0.144 |
| $\Delta14C$ (‰) | 0.233 | 0.035 |
| Depth | -0.191 | 0.011 |
| LOI | 0.265 | -0.008 |
| Alkyl | 0.284 | -0.041 |
| N-Alkyl/Methoxyl | -0.129 | -0.402 |
| O-Alkyl | -0.156 | -0.325 |
| Di_O_Alkyl | -0.273 | -0.027 |
| Aromatic | -0.251 | 0.034 |
| Phenolic | -0.230 | 0.296 |
| Amide/Carboxyl | 0.094 | 0.414 |
| Carbohydrate | -0.121 | -0.344 |
| Protein | 0.236 | -0.200 |
| Lignin | -0.264 | 0.157 |
| Lipid | 0.263 | -0.015 |
| Carbonyl | -0.005 | 0.464 |

Fig A5
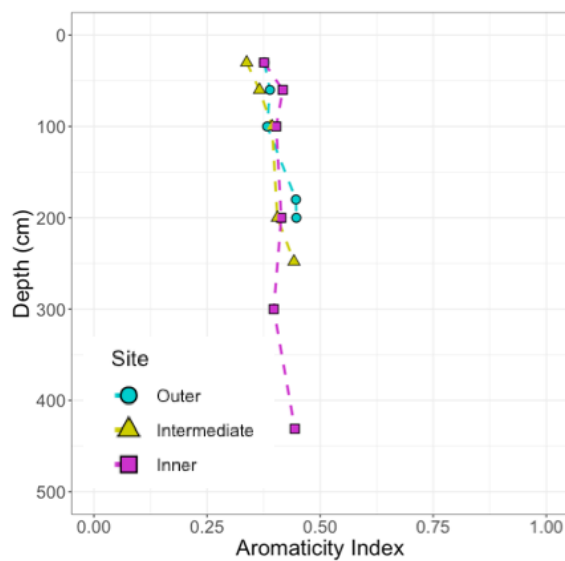
**Fig A5: Aromaticity Index. The aromaticity index has been used to describe decomposition state of soils. This index is expressed as the ratio of Aromatic-C to Alkyl + O-Alkyl + Aromatic C and is calculated using the results from integration of the $^{13}$C NMR spectra. As the aromaticity index approaches 1, the soil is considered more decomposed. The lack of change in aromaticity with depth, and the consistency across all three sites, suggests little decomposition has occurred over space and time. Sites are indicated by color and shape with blue circles indicating the outer site, yellow triangles the intermediate site, and pink squares the inner site.**

Fig A6
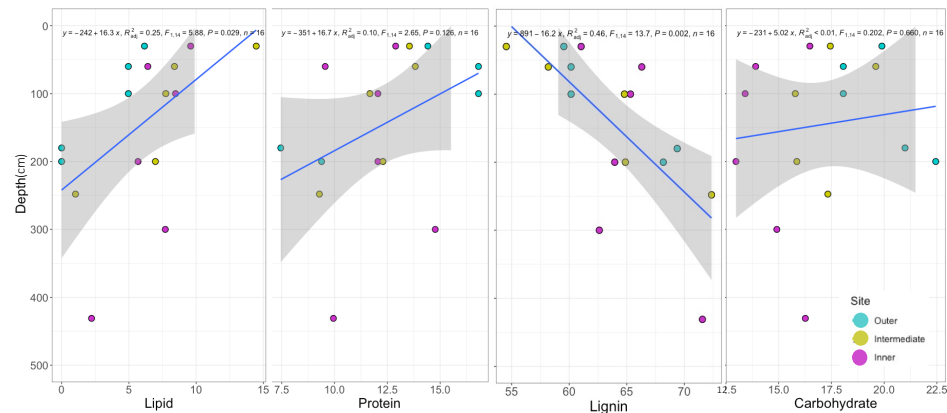
Fig A6: Linear regression of the four most abundant biomolecules from the mixing model versus depth. Sites have been pooled for this analysis but are indicated by color with blue indicating the outer site, yellow the intermediate site, and pink the inner site. Regressions show significant declines with depth for lipids, and significant increases with depth for lignin across sites.

**Author Contribution**

**Alexandra Hedgpeth**: Conceptualization; funding acquisition; data collection; formal analysis; investigation; methodology; visualization; writing – original draft. **Alison Hoyt:** Methodology; resources; formal analysis; visualization; supervision; writing – review and editing. **Daniela Cusack:** Conceptualization; funding acquisition; methodology; supervision; visualization; writing – review and editing. **Kyle Cavanaugh:** Supervision; writing – review and editing. **Karis McFarlane:** Funding acquisition; resources; methodology; supervision; writing – review and editing. Karis J. McFarlane and Daniela F. Cusack should be considered joint senior authors.

**Data Availability**

Following publication, the data that supports this manuscript will be publicly available at the US Department of Energy's Environmental Systems Science Data Infrastructure for a Virtual Ecosystem (ESS-DIVE: https://ess-dive.lbl.gov/) and will be submitted to the International Soil Radiocarbon Database (https://soilradiocarbon.org/).

**Competing interests**

The contact author has declared that none of the authors has any competing interests.

**Acknowledgements**

A. Hedgpeth thanks the Smithsonian Tropical Research Institute for a short-term research fellowship, Eric Brown for field support, and the staff at the Smithsonian Tropical Research Institute and the Bocas del Toro field station for logistical support. This project was supported in part by a University of California-National Lab In-Residence Graduate Fellowship (#L21GF3629) to A. Hedgpeth, which was hosted by Lawrence Livermore National Laboratory. The ^{13}C-NMR analysis for this work was supported under a U.S. Department of Energy User Award (#60514) to D. Cusack and A. Hedgpeth, which was conducted at the Environmental Molecular Sciences Laboratory. Access to field and lab sites in Panama was supported by DOE Office of Science Early Career Award DE-SC0015898 and NSF Geography & Spatial Studies Grant #BCS-1437591 to D. Cusack. We would like to thank Sarah Burton and Andrew Lipton from the Environmental Molecular Sciences Laboratory for their assistance with the ^{13}C-NMR analysis. A portion of this work was performed under the auspices of the U.S. Department of Energy by Lawrence Livermore National Laboratory under Contract DE-AC52-07NA27344 and funded by the U.S. Department of Energy Office of Science Early Career Program Award (#SCW1572) to K. McFarlane. We would like to thank Antonia L. Herwig, Lee Dietterich, and Makenna Brown for their assistance in the field.

**References**

Aliev, A. E.: Solid state NMR spectroscopy, in: Nuclear Magnetic Resonance, edited by: Hodgkinson, P., The Royal Society of Chemistry, 139–187, https://doi.org/10.1039/9781788010665-00139, 2020.

Anderson, J. A. R. and Muller, J.: Palynological study of a holocene peat and a miocene coal deposit from NW Borneo, Review of Palaeobotany and Palynology, 19, 291–351, https://doi.org/10.1016/0034-6667(75)90049-4, 1975.

635 Aravena, R., Warner, B. G., Charman, D. J., Belyea, L. R., Mathur, S. P., and Dinel, H.: Carbon Isotopic Composition of Deep Carbon Gases in an Ombrogenous Peatland, Northwestern Ontario, Canada, Radiocarbon, 35, 271–276, https://doi.org/10.1017/S0033822200064948, 1993.

Bader, C., Müller, M., Schulin, R., and Leifeld, J.: Peat decomposability in managed organic soils in relation to land use, organic matter composition and temperature, Biogeosciences, 15, 703–719, https://doi.org/10.5194/bg-15-703-2018, 2018.

Baldock, J. A., Masiello, C. A., Gélinas, Y., and Hedges, J. I.: Cycling and composition of organic matter in terrestrial and
640 marine ecosystems, Marine Chemistry, 92, 39–64, https://doi.org/10.1016/j.marchem.2004.06.016, 2004.

Barreto, C. and Lindo, Z.: Decomposition in Peatlands: Who Are the Players and What Affects Them?, Front. Young Minds, 8, 107, https://doi.org/10.3389/frym.2020.00107, 2020.

Beilman, D. W., Massa, C., Nichols, J. E., Elison Timm, O., Kallstrom, R., and Dunbar-Co, S.: Dynamic Holocene Vegetation and North Pacific Hydroclimate Recorded in a Mountain Peatland, Molokaʻi, Hawaiʻi, Front. Earth Sci., 7, 188,
645 https://doi.org/10.3389/feart.2019.00188, 2019.

Broek, T. A. B., Ognibene, T. J., McFarlane, K. J., Moreland, K. C., Brown, T. A., and Bench, G.: Conversion of the LLNL/CAMS 1 MV biomedical AMS system to a semi-automated natural abundance 14C spectrometer: system optimization and performance evaluation, Nuclear Instruments and Methods in Physics Research Section B: Beam Interactions with Materials and Atoms, 499, 124–132, https://doi.org/10.1016/j.nimb.2021.01.022, 2021.

650 Chanton, J. P., Glaser, P. H., Chasar, L. S., Burdige, D. J., Hines, M. E., Siegel, D. I., Tremblay, L. B., and Cooper, W. T.: Radiocarbon evidence for the importance of surface vegetation on fermentation and methanogenesis in contrasting types of boreal peatlands, Global Biogeochemical Cycles, 22, 2008GB003274, https://doi.org/10.1029/2008GB003274, 2008.

Charman, D. J., Aravena, R., Bryant, C. L., and Harkness, D. D.: Carbon isotopes in peat, DOC, CO2, and CH4 in a Holocene peatland on Dartmoor, southwest England, Geol, 27, 539, https://doi.org/10.1130/0091-
655 7613(1999)027<0539:CIIPDC>2.3.CO;2, 1999.

Chen, X., Xue, D., Wang, Y., Qiu, Q., Wu, L., Wang, M., Liu, J., and Chen, H.: Variations in the archaeal community and associated methanogenesis in peat profiles of three typical peatland types in China, Environmental Microbiome, 18, 48, https://doi.org/10.1186/s40793-023-00503-y, 2023.

Clymo, R. S., Turunen, J., and Tolonen, K.: Carbon Accumulation in Peatland, Oikos, 81, 368,
660 https://doi.org/10.2307/3547057, 1998.

Cobb, A. R., Hoyt, A. M., Gandois, L., Eri, J., Dommain, R., Abu Salim, K., Kai, F. M., Haji Suʼut, N. S., and Harvey, C. F.: How temporal patterns in rainfall determine the geomorphology and carbon fluxes of tropical peatlands, Proc. Natl. Acad. Sci. U.S.A., 114, https://doi.org/10.1073/pnas.1701090114, 2017.

Cohen, A. D., Raymond, R., Ramirez, A., Morales, Z., and Ponce, F.: The Changuinola peat deposit of northwestern Panama:
665 a tropical, back-barrier, peat(coal)-forming environment, International Journal of Coal Geology, 12, 157–192, https://doi.org/10.1016/0166-5162(89)90050-5, 1989.

Corbett, J. E.: DOC reactivity in a northern Minnesota peatland, Phd dissertation, 2012.

Corbett, J. E., Tfaily, M. M., Burdige, D. J., Cooper, W. T., Glaser, P. H., and Chanton, J. P.: Partitioning pathways of $CO_2$ production in peatlands with stable carbon isotopes, Biogeochemistry, 114, 327–340, https://doi.org/10.1007/s10533-012-9813-1, 2013.

Dargie, G. C., Lewis, S. L., Lawson, I. T., Mitchard, E. T. A., Page, S. E., Bocko, Y. E., and Ifo, S. A.: Age, extent and carbon storage of the central Congo Basin peatland complex, Nature, 542, 86–90, https://doi.org/10.1038/nature21048, 2017.

Dhandapani, S., Girkin, N. T., and Evers, S.: Spatial variability of surface peat properties and carbon emissions in a tropical peatland oil palm monoculture during a dry season, Soil Use and Management, 38, 381–395, https://doi.org/10.1111/sum.12741, 2022.

Dhandapani, S., Evers, S., Boyd, D., Evans, C. D., Page, S., Parish, F., and Sjogersten, S.: Assessment of differences in peat physico-chemical properties, surface subsidence and GHG emissions between the major land-uses of Selangor peatlands, CATENA, 230, 107255, https://doi.org/10.1016/j.catena.2023.107255, 2023.

Dommain, R., Cobb, A. R., Joosten, H., Glaser, P. H., Chua, A. F. L., Gandois, L., Kai, F., Noren, A., Salim, K. A., Su'ut, N. S. H., and Harvey, C. F.: Forest dynamics and tip-up pools drive pulses of high carbon accumulation rates in a tropical peat dome in Borneo (Southeast Asia), JGR Biogeosciences, 120, 617–640, https://doi.org/10.1002/2014JG002796, 2015.

Drollinger, S., Kuzyakov, Y., and Glatzel, S.: Effects of peat decomposition on $\delta^{13}C$ and $\delta^{15}N$ depth profiles of Alpine bogs, CATENA, 178, 1–10, https://doi.org/10.1016/j.catena.2019.02.027, 2019.

Farmer, J., Matthews, R., Smith, J. U., Smith, P., and Singh, B. K.: Assessing existing peatland models for their applicability for modelling greenhouse gas emissions from tropical peat soils, Current Opinion in Environmental Sustainability, 3, 339–349, https://doi.org/10.1016/j.cosust.2011.08.010, 2011.

Fritts, R.: Tropical Wetlands Emit More Methane Than Previously Thought, Eos, 103, https://doi.org/10.1029/2022EO220443, 2022.

Gandois, L., Teisserenc, R., Cobb, A. R., Chieng, H. I., Lim, L. B. L., Kamariah, A. S., Hoyt, A., and Harvey, C. F.: Origin, composition, and transformation of dissolved organic matter in tropical peatlands, Geochimica et Cosmochimica Acta, 137, 35–47, https://doi.org/10.1016/j.gca.2014.03.012, 2014.

Girkin, N. T., Turner, B. L., Ostle, N., Craigon, J., and Sjögersten, S.: Root exudate analogues accelerate $CO_2$ and $CH_4$ production in tropical peat, Soil Biology and Biochemistry, 117, 48–55, https://doi.org/10.1016/j.soilbio.2017.11.008, 2018.

Girkin, N. T., Vane, C. H., Cooper, H. V., Moss-Hayes, V., Craigon, J., Turner, B. L., Ostle, N., and Sjögersten, S.: Spatial variability of organic matter properties determines methane fluxes in a tropical forested peatland, Biogeochemistry, 142, 231–245, https://doi.org/10.1007/s10533-018-0531-1, 2019.

Girkin, N. T., Dhandapani, S., Evers, S., Ostle, N., Turner, B. L., and Sjögersten, S.: Interactions between labile carbon, temperature and land use regulate carbon dioxide and methane production in tropical peat, Biogeochemistry, 147, 87–97, https://doi.org/10.1007/s10533-019-00632-y, 2020.

Girkin, N. T., Cooper, H. V., Ledger, M. J., O'Reilly, P., Thornton, S. A., Åkesson, C. M., Cole, L. E. S., Hapsari, K. A., Hawthorne, D., and Roucoux, K. H.: Tropical peatlands in the Anthropocene: The present and the future, Anthropocene, 40, 100354, https://doi.org/10.1016/j.ancene.2022.100354, 2022.

Goldstein, A., Turner, W. R., Spawn, S. A., Anderson-Teixeira, K. J., Cook-Patton, S., Fargione, J., Gibbs, H. K., Griscom, B., Hewson, J. H., Howard, J. F., Ledezma, J. C., Page, S., Koh, L. P., Rockström, J., Sanderman, J., and Hole, D. G.: Protecting

705  irrecoverable carbon in Earth's ecosystems, Nat. Clim. Chang., 10, 287–295, https://doi.org/10.1038/s41558-020-0738-8, 2020.

Gruca-Rokosz, R. and Koszelnik, P.: Production pathways for CH4 and CO2 in sediments of two freshwater ecosystems in south-eastern Poland, PLoS ONE, 13, e0199755, https://doi.org/10.1371/journal.pone.0199755, 2018.

Hirano, T., Jauhiainen, J., Inoue, T., and Takahashi, H.: Controls on the Carbon Balance of Tropical Peatlands, Ecosystems, 710  12, 873–887, https://doi.org/10.1007/s10021-008-9209-1, 2009.

Hobbie, E. A. and Ouimette, A. P.: Controls of nitrogen isotope patterns in soil profiles, Biogeochemistry, 95, 355–371, https://doi.org/10.1007/s10533-009-9328-6, 2009.

Hodgkins, S. B., Richardson, C. J., Dommain, R., Wang, H., Glaser, P. H., Verbeke, B., Winkler, B. R., Cobb, A. R., Rich, V. I., Missilmani, M., Flanagan, N., Ho, M., Hoyt, A. M., Harvey, C. F., Vining, S. R., Hough, M. A., Moore, T. R., Richard, P. 715  J. H., De La Cruz, F. B., Toufaily, J., Hamdan, R., Cooper, W. T., and Chanton, J. P.: Tropical peatland carbon storage linked to global latitudinal trends in peat recalcitrance, Nat Commun, 9, 3640, https://doi.org/10.1038/s41467-018-06050-2, 2018.

Hornibrook, E. R. C., Longstaffe, F. J., and Fyfe, W. S.: Evolution of stable carbon isotope compositions for methane and carbon dioxide in freshwater wetlands and other anaerobic environments, Geochimica et Cosmochimica Acta, 64, 1013–1027, https://doi.org/10.1016/S0016-7037(99)00321-X, 2000a.

720  Hornibrook, E. R. C., Longstaffe, F. J., and Fyfe, W. S.: Factors Influencing Stable Isotope Ratios in CH 4 and CO 2 Within Subenvironments of Freshwater Wetlands: Implications for δ-Signatures of Emissions, Isotopes in Environmental and Health Studies, 36, 151–176, https://doi.org/10.1080/10256010008032940, 2000b.

Hoyos-Santillan, J.: 2014 Hoyos Controls of Carbon Turnover in Tropical Peatlands, https://doi.org/10.13140/2.1.3387.2329, 2014.

725  Hoyos-Santillan, J., Lomax, B. H., Large, D., Turner, B. L., Boom, A., Lopez, O. R., and Sjögersten, S.: Quality not quantity: Organic matter composition controls of CO2 and CH4 fluxes in neotropical peat profiles, Soil Biology and Biochemistry, 103, 86–96, https://doi.org/10.1016/j.soilbio.2016.08.017, 2016.

Hoyos-Santillan, J., Lomax, B. H., Large, D., Turner, B. L., Lopez, O. R., Boom, A., Sepulveda-Jauregui, A., and Sjögersten, S.: Evaluation of vegetation communities, water table, and peat composition as drivers of greenhouse gas emissions in lowland 730  tropical peatlands, Science of The Total Environment, 688, 1193–1204, https://doi.org/10.1016/j.scitotenv.2019.06.366, 2019.

Hoyt, A.: Methane production and transport in a tropical peatland, AGU Fall Meeting Abstracts, 2014.

Hoyt, A., Cadillo-Quiroz, H., Xu, X., Torn, M., Bazán Pacaya, A., Jacobs, M., Shapiama Peña, R., Ramirez Navarro, D., Urquiza-Muñoz, D., and Trumbore, S.: Isotopic Insights into Methane Production and Emission in Diverse Amazonian Peatlands, oral, https://doi.org/10.5194/egusphere-egu2020-12960, 2020.

735  Hoyt, A. M., Gandois, L., Eri, J., Kai, F. M., Harvey, C. F., and Cobb, A. R.: CO 2 emissions from an undrained tropical peatland: Interacting influences of temperature, shading and water table depth, Global Change Biology, 25, 2885–2899, https://doi.org/10.1111/gcb.14702, 2019.

Ingram, H. A. P.: Ecohydrology of Scottish peatlands, Transactions of the Royal Society of Edinburgh: Earth Sciences, 78, 287–296, https://doi.org/10.1017/S0263593300011226, 1987.

740 Jauhiainen, J., Takahashi, H., Heikkinen, J. E. P., Martikainen, P. J., and Vasander, H.: Carbon fluxes from a tropical peat swamp forest floor, Global Change Biology, 11, 1788–1797, https://doi.org/10.1111/j.1365-2486.2005.001031.x, 2005.

Kettridge, N., Turetsky, M. R., Sherwood, J. H., Thompson, D. K., Miller, C. A., Benscoter, B. W., Flannigan, M. D., Wotton, B. M., and Waddington, J. M.: Moderate drop in water table increases peatland vulnerability to post-fire regime shift, Sci Rep, 5, 8063, https://doi.org/10.1038/srep08063, 2015.

745 Kotsyurbenko, O. R., Chin, K.-J., Glagolev, M. V., Stubner, S., Simankova, M. V., Nozhevnikova, A. N., and Conrad, R.: Acetoclastic and hydrogenotrophic methane production and methanogenic populations in an acidic West-Siberian peat bog, Environ Microbiol, 6, 1159–1173, https://doi.org/10.1111/j.1462-2920.2004.00634.x, 2004.

Lähteenoja, O., Reátegui, Y. R., Räsänen, M., Torres, D. D. C., Oinonen, M., and Page, S.: The large A mazonian peatland carbon sink in the subsiding P astaza- M arañón foreland basin, P eru, Global Change Biology, 18, 164–178,
750 https://doi.org/10.1111/j.1365-2486.2011.02504.x, 2012.

Lampela, M., Jauhiainen, J., and Vasander, H.: Surface peat structure and chemistry in a tropical peat swamp forest, Plant Soil, 382, 329–347, https://doi.org/10.1007/s11104-014-2187-5, 2014.

Ledru, M.-P., Braga, P. I. S., Soubiès, F., Fournier, M., Martin, L., Suguio, K., and Turcq, B.: The last 50,000 years in the Neotropics (Southern Brazil): evolution of vegetation and climate, Palaeogeography, Palaeoclimatology, Palaeoecology, 123,
755 239–257, https://doi.org/10.1016/0031-0182(96)00105-8, 1996.

Li, D., Ni, H., Jiao, S., Lu, Y., Zhou, J., Sun, B., and Liang, Y.: Coexistence patterns of soil methanogens are closely tied to methane generation and community assembly in rice paddies, Microbiome, 9, 20, https://doi.org/10.1186/s40168-020-00978-8, 2021.

Liebner, S., Ganzert, L., Kiss, A., Yang, S., Wagner, D., and Svenning, M. M.: Shifts in methanogenic community composition
760 and methane fluxes along the degradation of discontinuous permafrost, Front. Microbiol., 6, https://doi.org/10.3389/fmicb.2015.00356, 2015.

Loisel, J., Gallego-Sala, A. V., Amesbury, M. J., Magnan, G., Anshari, G., Beilman, D. W., Benavides, J. C., Blewett, J., Camill, P., Charman, D. J., Chawchai, S., Hedgpeth, A., Kleinen, T., Korhola, A., Large, D., Mansilla, C. A., Müller, J., Van Bellen, S., West, J. B., Yu, Z., Bubier, J. L., Garneau, M., Moore, T., Sannel, A. B. K., Page, S., Väliranta, M., Bechtold, M.,
765 Brovkin, V., Cole, L. E. S., Chanton, J. P., Christensen, T. R., Davies, M. A., De Vleeschouwer, F., Finkelstein, S. A., Frolking, S., Gałka, M., Gandois, L., Girkin, N., Harris, L. I., Heinemeyer, A., Hoyt, A. M., Jones, M. C., Joos, F., Juutinen, S., Kaiser, K., Lacourse, T., Lamentowicz, M., Larmola, T., Leifeld, J., Lohila, A., Milner, A. M., Minkkinen, K., Moss, P., Naafs, B. D. A., Nichols, J., O'Donnell, J., Payne, R., Philben, M., Piilo, S., Quillet, A., Ratnayake, A. S., Roland, T. P., Sjögersten, S., Sonnentag, O., Swindles, G. T., Swinnen, W., Talbot, J., Treat, C., Valach, A. C., and Wu, J.: Expert assessment of future
770 vulnerability of the global peatland carbon sink, Nat. Clim. Chang., 11, 70–77, https://doi.org/10.1038/s41558-020-00944-0, 2021.

Malmer, N. and Holm, E.: Variation in the C/N-Quotient of Peat in Relation to Decomposition Rate and Age Determination with 210 Pb, Oikos, 43, 171, https://doi.org/10.2307/3544766, 1984.

McNicol, G., Knox, S. H., Guilderson, T. P., Baldocchi, D. D., and Silver, W. L.: Where old meets new: An ecosystem study
775 of methanogenesis in a reflooded agricultural peatland, Global Change Biology, 26, 772–785, https://doi.org/10.1111/gcb.14916, 2020.

Noon, M. L., Goldstein, A., Ledezma, J. C., Roehrdanz, P. R., Cook-Patton, S. C., Spawn-Lee, S. A., Wright, T. M., Gonzalez-Roglich, M., Hole, D. G., Rockström, J., and Turner, W. R.: Mapping the irrecoverable carbon in Earth's ecosystems, Nat Sustain, 5, 37–46, https://doi.org/10.1038/s41893-021-00803-6, 2021.

780 Norris, M. W., Turnbull, J. C., Howarth, J. D., and Vandergoes, M. J.: Pretreatment of Terrestrial Macrofossils, Radiocarbon, 62, 349–360, https://doi.org/10.1017/RDC.2020.8, 2020.

Nottingham, A. T., Bååth, E., Reischke, S., Salinas, N., and Meir, P.: Adaptation of soil microbial growth to temperature: Using a tropical elevation gradient to predict future changes, Global Change Biology, 25, 827–838, https://doi.org/10.1111/gcb.14502, 2019.

785 Ofiti, N. O. E., Schmidt, M. W. I., Abiven, S., Hanson, P. J., Iversen, C. M., Wilson, R. M., Kostka, J. E., Wiesenberg, G. L. B., and Malhotra, A.: Climate warming and elevated CO2 alter peatland soil carbon sources and stability, Nat Commun, 14, 7533, https://doi.org/10.1038/s41467-023-43410-z, 2023.

Omar, M. S., Ifandi, E., Sukri, R. S., Kalaitzidis, S., Christanis, K., Lai, D. T. C., Bashir, S., and Tsikouras, B.: Peatlands in Southeast Asia: A comprehensive geological review, Earth-Science Reviews, 232, 104149, 790 https://doi.org/10.1016/j.earscirev.2022.104149, 2022.

Osaki, M., Kato, T., Kohyama, T., Takahashi, H., Haraguchi, A., Yabe, K., Tsuji, N., Shiodera, S., Rahajoe, J. S., Atikah, T. D., Oide, A., Matsui, K., Wetadewi, R. I., and Silsigia, S.: Basic Information About Tropical Peatland Ecosystems, in: Tropical Peatland Eco-management, edited by: Osaki, M., Tsuji, N., Foead, N., and Rieley, J., Springer Singapore, Singapore, 3–62, https://doi.org/10.1007/978-981-33-4654-3_1, 2021.

795 Page, S. E., Rieley, J. O., and Banks, C. J.: Global and regional importance of the tropical peatland carbon pool, Global Change Biology, 17, 798–818, https://doi.org/10.1111/j.1365-2486.2010.02279.x, 2011.

Phillips, S. and Bustin, R. M.: Sedimentology of the Changuinola peat deposit: Organic and clastic sedimentary response to punctuated coastal subsidence, Geological Society of America Bulletin, 108, 794–814, https://doi.org/10.1130/0016-7606(1996)108<0794:SOTCPD>2.3.CO;2, 1996.

800 Phillips, S., Rouse, G. E., and Bustin, R. M.: Vegetation zones and diagnostic pollen profiles of a coastal peat swamp, Bocas del Toro, Panamá, Palaeogeography, Palaeoclimatology, Palaeoecology, 128, 301–338, https://doi.org/10.1016/S0031-0182(97)81129-7, 1997.

Ribeiro, K., Pacheco, F. S., Ferreira, J. W., De Sousa-Neto, E. R., Hastie, A., Krieger Filho, G. C., Alvalá, P. C., Forti, M. C., and Ometto, J. P.: Tropical peatlands and their contribution to the global carbon cycle and climate change, Global Change 805 Biology, 27, 489–505, https://doi.org/10.1111/gcb.15408, 2021.

Ruwaimana, M., Anshari, G. Z., Silva, L. C. R., and Gavin, D. G.: The oldest extant tropical peatland in the world: a major carbon reservoir for at least 47 000 years, Environ. Res. Lett., 15, 114027, https://doi.org/10.1088/1748-9326/abb853, 2020.

Sihi, D., Inglett, P. W., and Inglett, K. S.: Carbon quality and nutrient status drive the temperature sensitivity of organic matter decomposition in subtropical peat soils, Biogeochemistry, 131, 103–119, https://doi.org/10.1007/s10533-016-0267-8, 2016.

810 Sjögersten, S., Cheesman, A. W., Lopez, O., and Turner, B. L.: Biogeochemical processes along a nutrient gradient in a tropical ombrotrophic peatland, Biogeochemistry, 104, 147–163, https://doi.org/10.1007/s10533-010-9493-7, 2011.

Sugimoto, A. and Wada, E.: Carbon isotopic composition of bacterial methane in a soil incubation experiment: Contributions of acetate and, Geochimica et Cosmochimica Acta, 57, 4015–4027, https://doi.org/10.1016/0016-7037(93)90350-6, 1993.

Sun, C. L., Brauer, S. L., Cadillo-Quiroz, H., Zinder, S. H., and Yavitt, J. B.: Seasonal Changes in Methanogenesis and Methanogenic Community in Three Peatlands, New York State, Front. Microbio., 3, https://doi.org/10.3389/fmicb.2012.00081, 2012.

Troxler, T. G.: Patterns of phosphorus, nitrogen and $\delta^{15}N$ along a peat development gradient in a coastal mire, Panama, J. Trop. Ecol., 23, 683–691, https://doi.org/10.1017/S0266467407004464, 2007.

Troxler, T. G., Ikenaga, M., Scinto, L., Boyer, J. N., Condit, R., Perez, R., Gann, G. D., and Childers, D. L.: Patterns of Soil Bacteria and Canopy Community Structure Related to Tropical Peatland Development, Wetlands, 32, 769–782, https://doi.org/10.1007/s13157-012-0310-z, 2012.

United Nations Environment Programme, Global Environment Facility, Asia Pacific Network for Global Change Research, Global Environment Centre (Malaysia), and Wetlands International (Eds.): Assessment on peatlands, biodiversity, and climate change, Global Environment Centre & Wetlands International, Wageningen, Kuala Lumpur, 2 pp., 2008.

Upton, A., Vane, C. H., Girkin, N., Turner, B. L., and Sjögersten, S.: Does litter input determine carbon storage and peat organic chemistry in tropical peatlands?, Geoderma, 326, 76–87, https://doi.org/10.1016/j.geoderma.2018.03.030, 2018.

Wilson, R. M., Hopple, A. M., Tfaily, M. M., Sebestyen, S. D., Schadt, C. W., Pfeifer-Meister, L., Medvedeff, C., McFarlane, K. J., Kostka, J. E., Kolton, M., Kolka, R. K., Kluber, L. A., Keller, J. K., Guilderson, T. P., Griffiths, N. A., Chanton, J. P., Bridgham, S. D., and Hanson, P. J.: Stability of peatland carbon to rising temperatures, Nat Commun, 7, 13723, https://doi.org/10.1038/ncomms13723, 2016.

Wilson, R. M., Griffiths, N. A., Visser, A., McFarlane, K. J., Sebestyen, S. D., Oleheiser, K. C., Bosman, S., Hopple, A. M., Tfaily, M. M., Kolka, R. K., Hanson, P. J., Kostka, J. E., Bridgham, S. D., Keller, J. K., and Chanton, J. P.: Radiocarbon Analyses Quantify Peat Carbon Losses With Increasing Temperature in a Whole Ecosystem Warming Experiment, JGR Biogeosciences, 126, e2021JG006511, https://doi.org/10.1029/2021JG006511, 2021.

Wright, E. L., Black, C. R., Cheesman, A. W., Drage, T., Large, D., Turner, B. L., and Sjögersten, S.: Contribution of subsurface peat to $CO_2$ and $CH_4$ fluxes in a neotropical peatland: CARBON FLUXES IN A NEOTROPICAL PEATLAND, Global Change Biology, 17, 2867–2881, https://doi.org/10.1111/j.1365-2486.2011.02448.x, 2011.

Wright, E. L., Black, C. R., Turner, B. L., and Sjögersten, S.: Environmental controls of temporal and spatial variability in $CO_2$ and $CH_4$ fluxes in a neotropical peatland, Global Change Biology, 19, 3775–3789, https://doi.org/10.1111/gcb.12330, 2013.

Zhang, Y., Ma, A., Zhuang, G., and Zhuang, X.: The acetotrophic pathway dominates methane production in Zoige alpine wetland coexisting with hydrogenotrophic pathway, Sci Rep, 9, 9141, https://doi.org/10.1038/s41598-019-45590-5, 2019.